AMERICAN SOCIETY FOR MICROBIOLOGY | Journal of Virology

Next-Generation mRNA Sequencing Reveals Pyroptosis-Induced CD4$^+$ T Cell Death in Early Simian Immunodeficiency Virus-Infected Lymphoid Tissues

Wuxun Lu,[a,b] Andrew J. Demers,[a,b] Fangrui Ma,[a] Guobin Kang,[a,b] Zhe Yuan,[a,b] Yanmin Wan,[a,b,c] Yue Li,[a,b,d] Jianqing Xu,[c] Mark Lewis,[e] Qingsheng Li[a,b]

Nebraska Center for Virology[a] and School of Biological Sciences,[b] University of Nebraska—Lincoln, Lincoln, Nebraska, USA; Shanghai Public Health Clinical Center and Institutes of Biomedical Sciences, Fudan University, Shanghai, People's Republic of China[c]; College of Life Sciences, Nankai University, Tianjin, People's Republic of China[d]; BIOQUAL, Inc., Rockville, Maryland, USA[e]

ABSTRACT

Lymphoid tissues (LTs) are the principal sites where human immunodeficiency virus type 1 (HIV-1) replicates and virus-host interactions take place, resulting in immunopathology in the form of inflammation, immune activation, and CD4$^+$ T cell death. The HIV-1 pathogenesis in LTs has been extensively studied; however, our understanding of the virus-host interactions in the very early stages of infection remains incomplete. We investigated virus-host interactions in the rectal draining lymph nodes (dLNs) of rhesus macaques at different times after intrarectal inoculation (days postinoculation [dpi]) with simian immunodeficiency virus (SIV). At 3 dpi, 103 differentially expressed genes (DEGs) were detected using next-generation mRNA sequencing (RNA-seq). At 6 and 10 dpi, concomitant with increased SIV replication, 366 and 1,350 DEGs were detected, respectively, including upregulation of genes encoding proteins that play a role in innate antiviral immune responses, inflammation, and immune activation. Notably, genes (IFI16, caspase-1, and interleukin 1β [IL-1β]) in the canonical pyroptosis pathway were significantly upregulated in expression. We further validated increased pyroptosis using flow cytometry and found that the number of CD4$^+$ T cells expressing activated caspase-1 protein, the hallmark of ongoing pyroptosis, were significantly increased, which is correlated with decreased CD4$^+$ T cells in dLNs. Our results demonstrated that pyroptosis contributes to the CD4$^+$ T cell death *in vivo* in early SIV infection, which suggests that pyroptosis may play a pivotal role in the pathogenesis of SIV, and by extension, that of HIV-1, since pyroptosis not only induces CD4$^+$ T cell death but also amplifies inflammation and immune activation. Thus, blocking CD4$^+$ T cell pyroptosis could be a complementary treatment to antiretroviral therapy.

IMPORTANCE

Although secondary lymphoid tissues (LTs) are principal sites of human immunodeficiency virus type 1 (HIV-1) replication, inflammation, immune activation, and CD4$^+$ T cell death, immunopathogenesis in LTs during early infection remains largely unknown. Using the simian immunodeficiency virus (SIV)/rhesus monkey model of HIV rectal infection, we investigated early virus-host interactions. Our results revealed elevated potent host responses in early infection in LTs, including upregulation of genes involved in antiviral immune response, inflammation, and immune activation. Importantly, genes involved in the canonical pyroptosis pathway were significantly upregulated, and there was a strong correlation between CD4$^+$ T cell decrease and increased number of CD4$^+$ T cells expressing activated caspase-1 protein, demonstrating that pyroptosis contributes to CD4$^+$ T cell death *in vivo* in very early SIV infection. Our finding suggests that blocking pyroptosis may be able to decrease CD4$^+$ T cell loss during early SIV infection.

Secondary lymphoid tissues (LTs) are the principal sites where human immunodeficiency virus type 1 (HIV-1) replicates and host-virus interactions take place, resulting in immune activation, inflammation, CD4$^+$ T cell death, and ultimately immune deficiency (1–3). However, the mechanisms underlying immunopathogenesis in LTs during very early infection, especially CD4$^+$ T cell death, remain incompletely understood.

CD4$^+$ T cell death is a hallmark of disease progression in HIV-1 infection. To date, several mechanisms have been proposed to explain CD4$^+$ T cell death during HIV-1 infection in LTs. First, CD4$^+$ T cell death results directly from HIV-1 productive infection via viral cytopathic effect. However, only a small fraction of total CD4$^+$ T cells in LTs are productively infected by HIV-1 (4, 5); therefore, pathogenic effect alone is not sufficient to account for the overall CD4$^+$ T cell death *in vivo*. Another proposed mechanism is apoptosis in HIV-1 uninfected bystander CD4$^+$ T cells mediated through Fas and TRAIL (tumor necrosis factor [TNF]-related apoptosis-inducing ligand) signaling (6–8). It was also demonstrated that HIV-1 Gp120 protein, expressed on the mem-

Received 9 September 2015 **Accepted** 2 November 2015

Accepted manuscript posted online 11 November 2015

Citation Lu W, Demers AJ, Ma F, Kang G, Yuan Z, Wan Y, Li Y, Xu J, Lewis M, Li Q. 2016. Next-generation mRNA sequencing reveals pyroptosis-induced CD4$^+$ T cell death in early simian immunodeficiency virus-infected lymphoid tissues. J Virol 90:1080–1087. doi:10.1128/JVI.02297-15.

Editor: G. Silvestri

Address correspondence to Qingsheng Li, qli@unl.edu.

Supplemental material for this article may be found at http://dx.doi.org/10.1128/JVI.02297-15.

branes of infected cells or in soluble forms, can bind CD4 and CCR5 (chemokine [C-C motif] receptor 5)/CXCR4 (chemokine [C-X-C motif] receptor 4) of uninfected cells to induce apoptosis (9). Moreover, HIV-1 Tat, Vpr, and Nef proteins also can induce apoptosis of uninfected CD4$^+$ T cells (10–12). Additionally, cytotoxic CD8$^+$ T cells can lyse infected CD4$^+$ T cells (13). Last, a recent seminal study by Greene research group showed that pyroptosis is the major cause (95%) of death of HIV-1 nonproductively infected CD4$^+$ T cells (14), suggesting that CD4$^+$ T cell death, inflammation, and immune activation driven by pyroptosis make up a unified theme in the immunopathogenesis of HIV infection. However, the role of pyroptosis in CD4$^+$ T cell death *in vivo*, especially during early infection, remains largely unknown.

Pyroptosis resembles apoptotic programmed cell death but is a form of proinflammatory programmed cell death characterized by cell membrane rupture and release of inflammatory intracellular contents (15, 16). Pyroptosis can be induced by various microbial infections and noninfectious stimuli (17, 18). It was not initially distinguished from apoptosis, because both apoptosis and pyroptosis are self-destructive processes induced by activation of caspases, a group of cysteine proteases (19). However, further studies revealed that the mechanisms and characteristics of pyroptosis differ from those of apoptosis. Pyroptosis involves caspases-1, -4, and -5 and is inherently proinflammatory, whereas apoptosis involves caspase-2, -3, -6, -7, -8, -9, and -10 and occurs in the absence of inflammation (20). Although extensively studied in bacterial infections (21, 22), the roles of pyroptosis in viral infections were just recently recognized (14, 23). While the elegant *ex vivo* study demonstrated that pyroptosis induced by abortive HIV-1 infection is the predominant means of CD4$^+$ T cell depletion in HIV-1 infection (14), the *in vivo* role of pyroptosis in CD4$^+$ T cell death in HIV-1/simian immunodeficiency virus (SIV) infection, especially in very early infection, remains largely unknown. Pyroptosis not only can lead to cell death but it also induces inflammation and immune activation (24). Therefore, understanding the *in vivo* role of pyroptosis in driving vicious cycles of CD4$^+$ T cell death, inflammation, and immune activation in HIV pathogenesis is needed.

SIV infection of rhesus macaques recapitulates major aspects of mucosal transmission and immunopathogenesis of HIV-1 infection. Using an SIV/rhesus macaque model of HIV-1 rectal transmission, our recent study showed that there are robust rectal mucosal responses to acute SIV infection (25). However, host responses in LTs during very early infection are largely unknown. In this study, we used next-generation mRNA sequencing (RNA-seq) and found that draining lymph nodes (dLNs) of virus rectal entry had a significant response as early as 3 days after intrarectal inoculation (days postinoculation [dpi]) and more robust antiviral innate immune response, inflammation, and immune activation at 6 and 10 dpi. Importantly, our transcriptome data unbiasedly revealed significant upregulation in expression of many genes in the signaling pathway of pyroptosis. Furthermore, pyroptosis in CD4$^+$ T cells was verified using flow cytometry.

In all, our data show there is a significant increase of pyroptosis in CD4$^+$ T cells in LTs, which correlates with a decline in CD4$^+$ T cells, and increases of inflammation and immune activation during early SIV infection. Thus, we unambiguously demonstrate, for the first time to our knowledge, that pyroptosis contributes to *in vivo* CD4$^+$ T cell death in LTs during early SIV infection. Further study is warranted to develop therapeutic measures targeting pyroptosis in order to simultaneously block CD4$^+$ T cell death, reduce inflammation, and decrease immune activation as a complementary treatment to antiretroviral therapy.

MATERIALS AND METHODS

Rhesus macaques and SIV rectal inoculation. This study was reviewed and approved by the Institutional Animal Care and Use Committee (IACUC) at the University of Nebraska—Lincoln (protocol number 559) and BIOQUAL, Inc. (protocol number 10-0000-01). Twenty-two adult male rhesus macaques (*Macaca mulatta*) of Indian origin housed at BIOQUAL, Inc., in accordance with the regulations of the American Association for Accreditation of Laboratory Animal Care standards were used in this study. All these animals tested negative for HIV-2, SIV, type D retrovirus, and simian type D retrovirus 1 (SRV-1) infections. The macaques were intrarectally inoculated with SIVmac251 (3.4×10^4 50% tissue culture infective doses [$TCID_{50}$], provided by Nancy Miller, NIAID, NIH). For the RNA-seq study, draining lymph node (dLN) tissues from macaques at day 0 (uninfected; $n = 3$), 3 ($n = 3$), 6 ($n = 4$), and 10 ($n = 3$) postinoculation were used. For quantification of CD4$^+$ T cells and activated caspase-1 level using flow cytometry, more macaques at days 0 (uninfected; $n = 3$), 14 ($n = 3$), and 28 ($n = 3$) postinoculation were added. A portion of dLNs were snap-frozen in liquid nitrogen immediately after collection and stored at −80°C until they were analyzed, and another portion was immediately used for lymphocyte isolation.

RNA extraction and next-generation sequencing. Total RNA was extracted according to our previously published protocol (26). Briefly, dLNs were homogenized in TRIzol (catalog no. 15596-018; Invitrogen) with a power homogenizer for total RNA extraction. The extracted RNA samples were further purified using the RNeasy minikit (catalog no. 74104; Qiagen). RNA quality was verified by using a Bioanalyzer 2100 (Agilent, Palo Alto, CA), and RNA-seq libraries were generated using the Sample Prep kit (catalog no. FC-122-1001; Illumina Inc.) according to the manufacturer's instructions. Briefly, mRNA was purified from total RNA using oligo(dT) magnetic beads, fragmented, and reverse transcribed into cDNA, which went through an end-repair process followed by ligation to adapters. A single DNA fragment was enriched by PCR and used for sequencing on an Illumina Genome Analyzer IIx sequencer at the Genomics Core Research Facility of the University of Nebraska—Lincoln. Each of the 13 sequenced samples had approximately 30 million 75-nucleotide single-end reads, and the sequencing results passed quality control.

Transcriptome data analyses. Reads from each sample were mapped to the rhesus macaque genome (Mmul_051212) and SIVmac251 full-length reference sequences using GSNAP program (27) with default parameters, and the resulting SAM (sequence alignment/map) files were converted to BAM (binary version of SAM) files using SAMtools (28). Integrative Genomics Viewer (IGV) (29) was used for visualization and quality check of mapping. For rhesus transcriptome analysis, Java Picard utilities were used to count the number of reads mapped to each gene annotated in the rhesus macaque reference genome. The read count data for each annotated gene were then statistically analyzed using the DESeq package, which implements an extended negative binomial distribution model (30). Compared with genes in uninfected control macaques, genes in SIV-infected samples with an adjusted *P* value (Benjamini-Hochberg method) (30) lower than 0.05 and a fold change greater than two were defined as differentially expressed genes (DEGs), which were further analyzed for gene functional categorization and pathway activation by using DAVID (31) and literature search. To analyze the level of SIV mRNA, reads mapped to the SIVmac251 reference sequence were counted base by base using SAMtools. The count data were normalized based on 30 million mapped reads in each sample, averaged, and plotted.

Flow cytometry. To quantify CD4$^+$ T cells and their pyroptosis, the rhesus macaques euthanized at 10, 14, and 28 dpi and uninfected controls were studied. Lymphocytes freshly isolated from dLNs were stained with antibodies against human CD3 (Alexa Fluor 700 conjugated; catalog no. 557917; BD Pharmingen), CD4 (phycoerythrin [PE]-Cy5.5 conjugated;

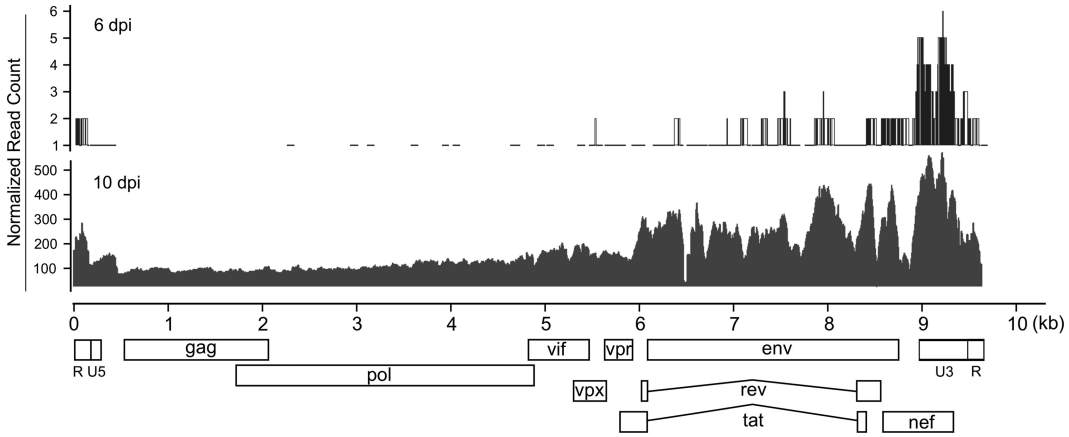

FIG 1 Genome-wide SIV gene expression quantified using RNA-seq. The read coverage values on the SIV genome were normalized based on 30 million reads mapped to rhesus macaque and SIV genomes.

catalog no. 35-0048-42; eBioscience) and 6-carboxyfluorescein (FAM)-YVAD-fluoromethylketone (FMK) (catalog no. 97; ImmunoChemistry Technologies). FAM-YVAD-FMK can bind to activated caspase-1, a marker of ongoing pyroptosis (32). The samples were run on an Aria II cell sorter (BD Company, Franklin Lakes, NJ). The collected data were analyzed using FlowJo (FlowJo LLC, Ashland, OR).

Statistical analysis. The DESeq package, which implements an extended negative binomial distribution model (30), was used to analyze read count data of each gene in the rhesus macaque genome to identify differentially expressed genes (DEGs). In flow cytometric result analysis, nonparametric Mann-Whitney U test was conducted using R scripts. A P value of ≤ 0.05 was considered significant. To test the relationship of activated caspase-1 in $CD4^+$ T cells and $CD4^+$ T cell counts, the Pearson correlation coefficient was calculated.

Microarray data accession number. The raw sequence data were deposited in the Sequence Read Archive (SRA) of the National Center for Biotechnology Information (NCBI) under accession number SRP056872.

RESULTS

SIV productive infection in dLNs at different days after rectal inoculation. To identify the genome-wide gene expression pattern of SIV, viral mRNA reads were mapped to the SIV genome, the read coverage at each position was calculated, and the data were then normalized and plotted (Fig. 1), which provided unprecedented detail of SIV mRNA transcripts with single-nucleotide resolution. At 3 days after rectal inoculation (days postinoculation [dpi]), SIV mRNA was detected in the dLNs using RNA-seq, albeit with low read coverage, which is consistent with the results of quantitative reverse transcription-PCR (qRT-PCR) and *in situ* hybridization (ISH) (unpublished data). At 6 and 10 dpi, significantly higher SIV mRNA was detected in the dLNs using RNA-seq and viral RNA (vRNA) levels increased 100-fold from 6 dpi to 10 dpi (Fig. 1). The level of expression of different SIV genes varied, with accessory protein genes expressed higher than *gag* and *pol* genes, which may help antagonize host antiviral restriction factors discussed below (see Fig. S1 in the supplemental material).

Robust host responses to early SIV infection in dLNs. To elucidate host responses in dLNs during very early SIV infection, the RNA-seq reads were mapped to each gene in the rhesus macaque genome, counted, and statistically analyzed. As shown in Fig. 2A and Table S1 in the supplemental material, there were 103, 366, and 1,350 DEGs at 3, 6, and 10 dpi, respectively. This increased number of DEGs correlated with the levels of SIV RNA at 3, 6, and 10 dpi. To understand their functions, the DEGs were categorized by using DAVID based on their adjusted P values (31). There was no significantly enriched category at 3 dpi. However, there were multiple enriched functional categories at 6 dpi and more at 10 dpi, including cytosolic DNA sensing, Toll-like receptor signaling, retinoic acid-inducible gene I (RIG-I)-like receptor signaling, chemokine signaling (Fig. 2B), immune activation, and pyroptosis as shown in the respective sections below.

Activation of pattern recognition receptors. In the enriched functional categories at 6 dpi, cytosolic DNA sensing, Toll-like receptor signaling, and RIG-I receptor signaling for recognition of foreign pathogens were detected, indicating that SIV was sensed, through which immune responses were initiated. For clarity, DEGs of pattern recognition of pathogens and interferon signaling pathways were illustrated (Fig. 2C). At 6 dpi, RIG-I, melanoma differentiation-associated protein 5 (MDA5), LGP2 and DDX60, all involved in double-stranded RNA (dsRNA) recognition, were upregulated. At 10 dpi, additionally, the levels of expression of Toll-like receptor 3 (TLR3), TLR7, and TLR8 were significantly upregulated, of which TLR3 recognizes dsRNA in endosomes, and TLR7 and TLR8 recognize single-stranded RNA (ssRNA) in endosomes (33).

After HIV-1/SIV entry, the ssRNA genome is used as a template to synthesize its cDNA. The presence of DNA in eukaryotic cell cytoplasm is a danger signal that triggers defense responses (34). The upregulated genes in cytosolic DNA recognition at 10 dpi include DLM-1/ZBP1 (DAI), cyclic GMP-AMP synthase (cGAS), and IFI16 (Fig. 2C), reflecting host responses to the presence of SIV DNA. After sensing HIV-1 and other retroviruses, cGAS can induce type I interferons and cytokines (35), and IFI16 can control HIV-1 replication (36). In addition to viral recognition, our results showed the upregulation of genes involved in bacterial recognition (TLR2, TLR4, and caspase-4 and -5) (37, 38) at 10 dpi.

Elevated antiviral responses. The antiviral activities of alpha interferon (IFN-α) and IFN-β are exerted through induction of a large number of interferon-stimulated genes (ISGs). At 6 and 10 dpi, numerous ISGs were upregulated in expression. For clarity, the ISGs were classified based on their functions (see Fig. S1 in the supplemental material). It is striking that these

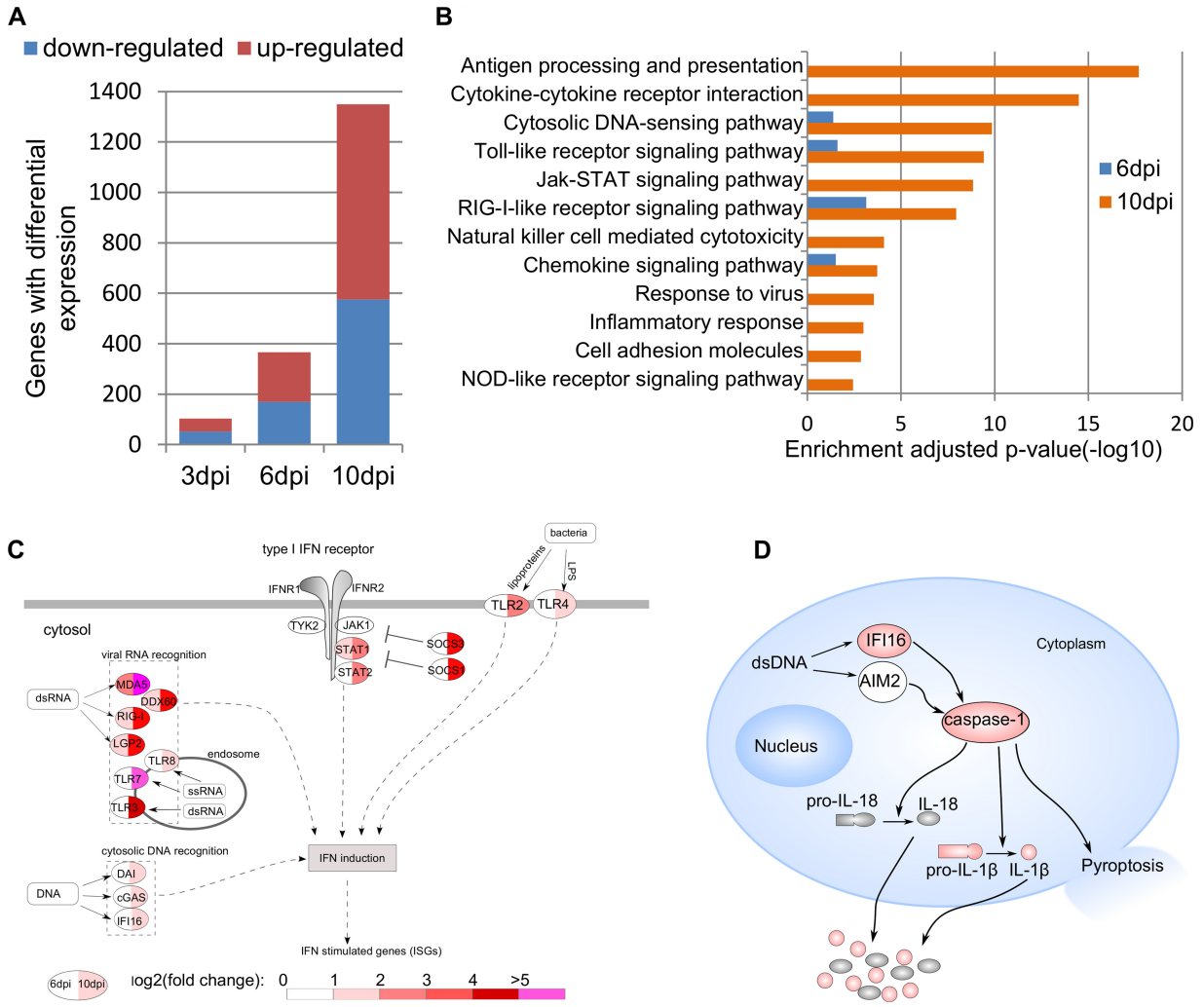

FIG 2 Robust host responses in dLNs during early SIV infection. (A) Number of differentially expressed genes (DEGs) at 3, 6, and 10 dpi. (B) Enriched functional categories of DEGs at 6 dpi and 10 dpi. (C) DEGs involved in interferon signaling pathways. (D) Schematic representation of canonical pyroptosis pathway. The DEGs at 10 dpi are shown in red.

upregulated ISGs target various steps of the HIV-1/SIV life cycle, i.e., inhibition of viral entry (IFITM1 and IFITM3); blockade of viral disassembly (TRIM5); introduction of hypermutations (APOBEC3A, APOBEC3C, APOBEC3D, APOBEC3F, APOBEC3G, and APOBEC3H); blockade of viral DNA synthesis (SAMHD1 and MOV10); inhibition of viral transcription (MX1, MX2, PML, and SP100); degradation of mRNA (OAS1, OAS2, OAS3, and OASL); inhibition of protein translation (SLFN13, SLFN14, PKR, and IFIT protein family); blockade of viral Gag protein trafficking (TRIM22); blockade of viral assembly (HERC5 and HERC6); and blockade of viral release (ISG15, BST2/tetherin, and viperin). Other upregulated ISGs (e.g., IFI44L and IFI6) also belong to viral restriction factors, but the inhibitory mechanisms are unclear.

Besides ISGs, the upregulated DEGs also showed enrichment of antigen presentation, with upregulated expression of major histocompatibility complex (MHC) class I α-chain, β-chain (B2M), TAP1, and TAP1-binding protein (TAP1BP) at 10 dpi. Furthermore, upregulated DEGs also include CD94 (KLRD1), perforin (PRF1), KIR2DL4, FcgRIII (FCGR3), and IFN-γ, indicating the activation of NK cell-mediated cytotoxicity (Fig. 2B).

Immune activation and inflammation. Immune activation and inflammation stimulated by foreign pathogens through pattern recognition receptors as discussed above manifest increased expression of ISGs and proinflammatory chemokines and cytokines. As shown in Table S1 in the supplemental material, RNA-seq revealed, as early as 3 dpi, that CCL13 and CCL20 were significantly upregulated. At 6 dpi, CXCR3 ligands chemokine (C-X-C motif) ligand 9 (CXCL9), CXCL10, and CXCL11 were upregulated. At 10 dpi, a larger number of cytokine genes were upregulated, including chemokine (C-C motif) ligand 3 CCL3 (macrophage inflammatory protein 1α [MIP-1α]), CCL5 (RANTES), IL-10, IL-1β, IFN-α, IFN-β, and IFN-γ.

CD4+ T cell death. CD4 T cell death in LTs is a hallmark of HIV-1 infection. As expected and as reported previously (26, 39, 40), RNA-seq revealed an upregulated expression of genes involved in apoptosis, including FasL and TNF-related apoptosis-inducing ligand (TRAIL). Importantly, genes involved in canon-

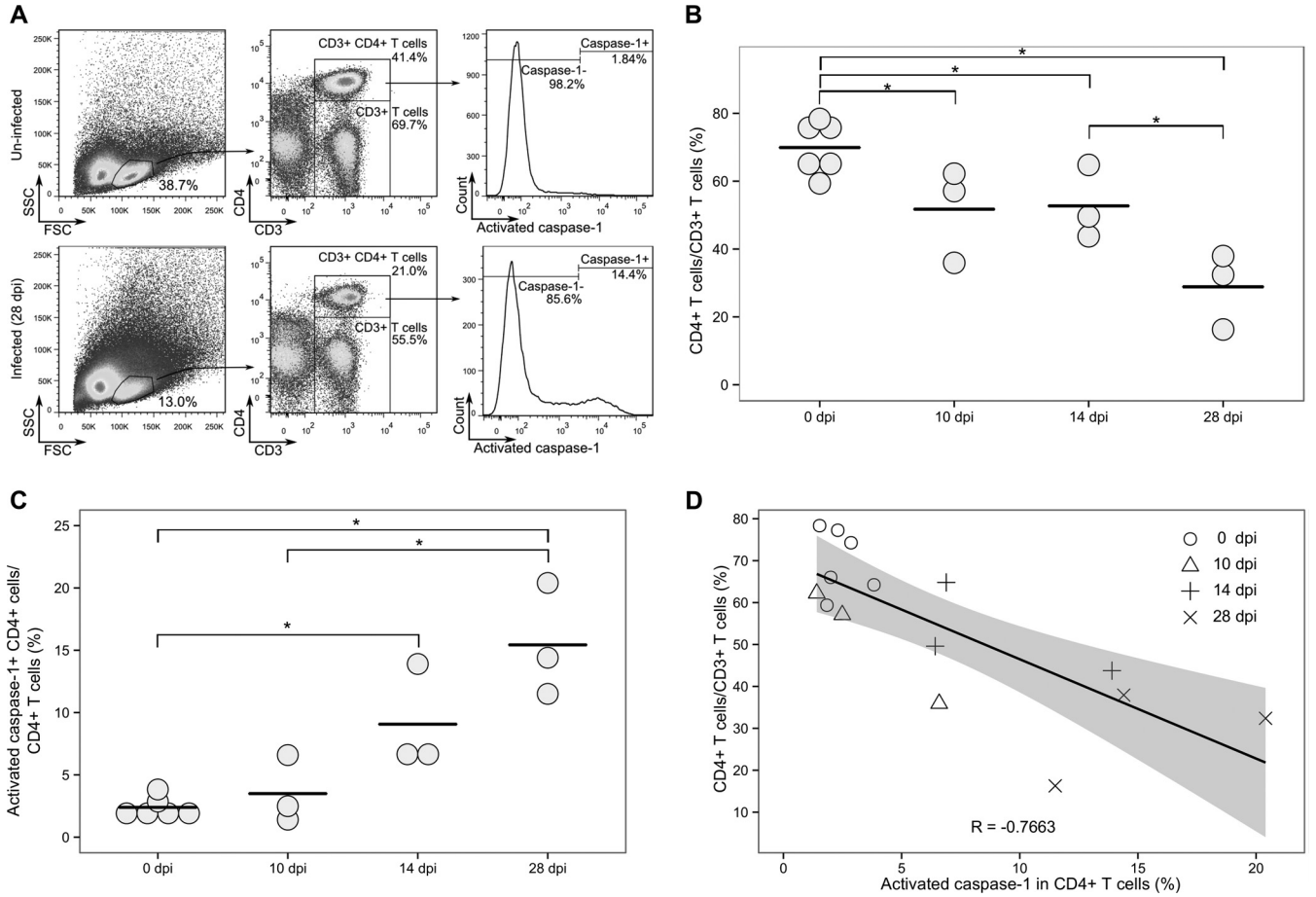

FIG 3 $CD4^+$ T cell pyroptosis correlates with decline of $CD4^+$ T cells assessed using flow cytometry. (A) Representative results of $CD4^+$ T cells expressing active caspase-1 protein in dLNs of uninfected macaques and macaques 28 dpi. FSC, forward scatter: SSC, side scatter. (B) Decrease of $CD4^+$ T cells in dLNs after SIV infection. (C) Increase of $CD4^+$ T cells expressing activated caspases-1 in dLNs after SIV inoculation. In panels B and C, each symbol represents the value for an individual macaque, and each bar shows the average value for the group of macaques. Mean values that are significantly different ($P \leq 0.05$) are indicated by a bar and asterisk. (D) Correlation analysis of $CD4^+$ T cells expressing activated caspase-1 and the levels of $CD4^+$ T cells.

ical pyroptosis were also upregulated (Fig. 2D). There was an upregulated expression of caspase-1 and IL-1β genes, the former is the hallmark of canonical pyroptosis, indicating there is an ongoing pyroptosis in LTs during early SIV infection. Since the *in vivo* role of pyroptosis during HIV-1/SIV infection remains poorly defined, we quantified $CD4^+$ T cell pyroptosis in dLNs of infected and uninfected macaques by measuring activated caspase-1 in $CD4^+$ T cells using flow cytometry (Fig. 3A and C). The mean of $CD4^+$ T cells expressing activated caspase-1 increased 1.5-fold at 10 dpi compared with uninfected macaques, although it does not reach statistical significance (Fig. 3C). At 14 and 28 dpi, the mean of $CD4^+$ cells expressing activated caspase-1 significantly increased 3.8- and 6.4-fold, respectively ($P < 0.05$).

In the quantification of $CD4^+$ T cells, $CD4^+$ T cells out of $CD3^+$ T cells significantly declined from 70% in uninfected animals to 51.7% at 10 dpi and further decreased to 28.9% at 28 dpi (Fig. 3B). This dramatic decrease is consistent with the results of a previous study (41). To test the relationship between $CD4^+$ T cell loss and pyroptosis of $CD4^+$ T cells, a linear regression was performed, and Pearson correlation coefficient was calculated. The correlation coefficient ($R = -0.7663$) indicated a strong negative correlation between activated caspase-1 in $CD4^+$ T cells and $CD4^+$ T cell decline. The coefficient of determination ($R^2 = 0.5872$) further suggested that activated caspase-1 expression in $CD4^+$ T cells partially (58.7%) accounts for the $CD4^+$ T cell decline. Therefore, our results show that there is an increased pyroptosis-mediated $CD4^+$ T cell death in LTs in early SIV infection.

DISCUSSION

HIV-1 immunopathogenesis mainly takes place in the secondary LTs. Accumulated evidence shows that inflammation, immune activation, and $CD4^+$ T cell death resulting from HIV-1 infection are three major themes in LTs driving disease progression (3, 42). In this study, we systematically investigated virus-host interactions in LTs during very early infection using an SIV/Indian rhesus macaque model of HIV-1 rectal infection. At 3 dpi, RNA-seq analyses revealed 103 DEGs in draining LNs, indicating a rapid host response to the fast SIV dissemination into dLNs following rectal transmission. A recent study demonstrated that rhesus macaques receiving daily potent combined antiretroviral therapy (ART), initiated 3 days after intrarectal inoculation of SIVmac251, controlled viremia to an undetectable level for 6 months. However, after interruption of ART, viremia rebounded in all macaques (43). Consistent with

this observation, our results of clear host responses in dLNs by RNA-seq demonstrated that SIV has disseminated into dLNs and established a productive infection at 3 dpi. Over the course of SIV infection from 6 to 10 dpi, there was a 100-fold increase of viral mRNA in dLNs detected by RNA-seq (Fig. 1); and the host responses were concurrently increased, from 366 to 1,350 DEGs. The DEGs at 6 and 10 dpi show increased inflammation and immune activation manifested as increased expression of pathogen pattern recognition receptors (PRRs), ISGs, cytokines, and chemokines, such as CCL3 (MIP-1α), CCL5 (RANTES), IL-10, IL-1β, IFN-α, IFN-β, and IFN-γ.

The host inflammation, immune activation, and antiviral responses are initiated by activation of PRRs. Our results showed PRRs of cytosolic DNA sensing, Toll-like receptor signaling, and RIG-I-like receptor signaling were upregulated both at 6 dpi and at 10 dpi. NOD-like receptor signaling was significantly enriched at 10 dpi (Fig. 2B). Viral RNA recognition receptors, including RIG-I (3-fold), MDA5 (2.6-fold), LGP2 (3-fold), and DDX60 (3.8-fold), were upregulated from 6 dpi, and genes encoding these proteins were further upregulated at 10 dpi (Fig. 2C). RIG-I, MDA5, and LGP2 are key receptors that trigger interferon expression after RNA virus infection (44). The upregulation of the RNA-sensing genes and detected SIV RNA suggest that major host responses to the presence of SIV in LTs are initiated at or before 6 dpi. Besides RNA sensing, genes encoding cytosolic DNA sensors were also upregulated, including DAI (2.9-fold), cGAS (2.4-fold), and IFI16 (2.4-fold) at 10 dpi, which are also upstream of the canonical pyroptosis pathway.

CD4$^+$ T cell death in LTs is one of the consequences of HIV-1 infection. In this study, the average frequency of CD4$^+$ T cells (percentage of CD4$^+$ T cells out of CD3$^+$ T cells) decreased at 10 dpi as measured by flow cytometry (Fig. 3B). With regard to the mechanism of CD4$^+$ T cell decline, RNA-seq results show a significantly increased expression of apoptosis genes of FasL (5-fold) and TRAIL (2.6-fold) at 10 dpi, indicating ongoing apoptosis in LTs, which is consistent with our and other's previous reports showing that the activated Fas/FasL pathway contributes to CD4$^+$ T cell death in HIV-1 and SIV infection (26, 39, 40). Importantly, genes involved in pyroptosis (IFI16, caspase-1, and IL-1β) were significantly upregulated (Fig. 2D), suggesting that pyroptosis also contributes to CD4$^+$ T cell death *in vivo* in early SIV infection. Flow cytometric study of lymphocytes freshly isolated from the same dLNs showed that the percentage of CD4$^+$ T cells that expressed active caspase-1 protein increased during early SIV infection compared with uninfected controls. The percentage of CD4$^+$ T cells expressing activated caspase-1 protein at 10 dpi was higher than that for the controls but did not reach statistical significance, although caspase-1 mRNA at 10 dpi was already significantly upregulated in dLNs. This discrepancy may reflect the different regulatory mechanisms and kinetics of mRNA versus protein expression. However, the percentage of CD4$^+$ T cells expressing activated caspase-1 protein significantly increased at 14 and 28 dpi. Furthermore, there is a strong negative correlation between increased expression of active caspase-1 in CD4$^+$ T cells and the decline of CD4$^+$ T cells. The coefficient of determination suggests that pyroptosis contributes to more than half (58.7%) of CD4$^+$ T cell loss during early SIV infection. The remaining CD4$^+$ T cell loss might be mediated by apoptosis and other mechanisms as discussed above. Of note, in addition to increased expression of caspase-1, which is involved in canonical pyroptosis, our RNA-seq results also revealed increased expression of caspase-4 and caspase-5 of the noncanonical pyroptosis pathway. The noncanonical pyroptosis pathway can be activated by intracellular lipopolysaccharide (LPS) (38), the major structural element of the outer membrane in Gram-negative bacteria. The plasma LPS level was elevated in HIV-1 chronically infected individuals and SIV chronically infected rhesus macaques (45, 46). Recently, it was also documented that 14 and 28 days after SIV infection, the gut epithelial barrier was compromised (47, 48), and LPS levels in the colon and mesenteric lymph nodes were significantly increased in rhesus macaques (48). Considering the damage to the intestinal epithelial barrier, microbial translocation in SIV infection, and the increased expression of caspase-4, caspase-5, and bacterial recognition receptor TLR2 and TLR4 genes revealed in this study, noncanonical pyroptosis may also contribute to CD4$^+$ T cell death *in vivo* during early SIV infection. However, further studies are required to further examine this hypothesis.

Collectively, our study demonstrates a striking pattern of host responses to early SIV infection in LTs characterized by upregulation of gene expression of antivirus, inflammation, immune activation, and CD4$^+$ T cell death. Importantly, to our knowledge, this is the first *in vivo* study to demonstrate that canonical pyroptosis contributes to CD4$^+$ T cells death *in vivo* in LTs during early SIV infection. Since pyroptosis can drive a vicious cycle of CD4$^+$ T cell death, proinflammatory cytokine release, and intensified immune activation, blocking pyroptosis could be a complementary treatment to antiretroviral therapy.

ACKNOWLEDGMENTS

We thank all of the macaque care and veterinary staff at BIOQUAL, Inc. We thank Yuannan Xia and Mei Chen at the Genomics Core Research Facility, University of Nebraska—Lincoln (UNL), for mRNA-seq services, and Christian Elowsky and You Zhou at the Microscopic Core Research Facility, UNL, for assistance with confocal imaging.

This work was supported by National Institutes of Health grant R01 DK087625 (to Q. Li) and by Preclinical Research & Development Branch, VRP, DAIDS, NIAID, NIH, Task Order under N01-AI-30018 (to Q. Li). Yue Li was supported by the Fogarty International Center grant at the University of Nebraska—Lincoln (D43 TW001429).

The funders had no role in study design, data collection, and interpretation or the decision to submit the work for publication.

FUNDING INFORMATION

HHS | National Institutes of Health (NIH) provided funding to Qingsheng Li under grant number R01 DK087625.

REFERENCES

1. **Fox CH, Tenner-Racz K, Racz P, Firpo A, Pizzo PA, Fauci AS.** 1991. Lymphoid germinal centers are reservoirs of human immunodeficiency virus type 1 RNA. J Infect Dis **164:**1051–1057. http://dx.doi.org/10.1093/infdis/164.6.1051.
2. **Pantaleo G, Graziosi C, Butini L, Pizzo PA, Schnittman SM, Kotler DP, Fauci AS.** 1991. Lymphoid organs function as major reservoirs for human immunodeficiency virus. Proc Natl Acad Sci U S A **88:**9838–9842. http://dx.doi.org/10.1073/pnas.88.21.9838.
3. **Meyaard L, Otto SA, Jonker RR, Mijnster MJ, Keet RP, Miedema F.** 1992. Programmed death of T cells in HIV-1 infection. Science **257:**217–219. http://dx.doi.org/10.1126/science.1352911.
4. **Embretson J, Zupancic M, Ribas JL, Burke A, Racz P, Tenner-Racz K, Haase AT.** 1993. Massive covert infection of helper T lymphocytes and

macrophages by HIV during the incubation period of AIDS. Nature **362:** 359–362. http://dx.doi.org/10.1038/362359a0.
5. **Doitsh G, Cavrois M, Lassen KG, Zepeda O, Yang Z, Santiago ML, Hebbeler AM, Greene WC.** 2010. Abortive HIV infection mediates CD4 T cell depletion and inflammation in human lymphoid tissue. Cell **143:** 789-801. http://dx.doi.org/10.1016/j.cell.2010.11.001.
6. **Finkel TH, Tudor-Williams G, Banda NK, Cotton MF, Curiel T, Monks C, Baba TW, Ruprecht RM, Kupfer A.** 1995. Apoptosis occurs predominantly in bystander cells and not in productively infected cells of HIV- and SIV-infected lymph nodes. Nat Med **1:**129–134. http://dx.doi.org/10.1038/nm0295-129.
7. **Badley AD, McElhinny JA, Leibson PJ, Lynch DH, Alderson MR, Paya CV.** 1996. Upregulation of Fas ligand expression by human immunodeficiency virus in human macrophages mediates apoptosis of uninfected T lymphocytes. J Virol **70:**199–206.
8. **Herbeuval JP, Nilsson J, Boasso A, Hardy AW, Kruhlak MJ, Anderson SA, Dolan MJ, Dy M, Andersson J, Shearer GM.** 2006. Differential expression of IFN-alpha and TRAIL/DR5 in lymphoid tissue of progressor versus nonprogressor HIV-1-infected patients. Proc Natl Acad Sci U S A **103:**7000–7005. http://dx.doi.org/10.1073/pnas.0600363103.
9. **Perfettini JL, Castedo M, Roumier T, Andreau K, Nardacci R, Piacentini M, Kroemer G.** 2005. Mechanisms of apoptosis induction by the HIV-1 envelope. Cell Death Differ **12**(Suppl 1):S916–S923.
10. **Li CJ, Friedman DJ, Wang C, Metelev V, Pardee AB.** 1995. Induction of apoptosis in uninfected lymphocytes by HIV-1 Tat protein. Science **268:** 429–431. http://dx.doi.org/10.1126/science.7716549.
11. **Stewart SA, Poon B, Jowett JB, Chen IS.** 1997. Human immunodeficiency virus type 1 Vpr induces apoptosis following cell cycle arrest. J Virol **71:**5579–5592.
12. **Lenassi M, Cagney G, Liao M, Vaupotic T, Bartholomeeusen K, Cheng Y, Krogan NJ, Plemenitas A, Peterlin BM.** 2010. HIV Nef is secreted in exosomes and triggers apoptosis in bystander CD4+ T cells. Traffic **11:** 110–122. http://dx.doi.org/10.1111/j.1600-0854.2009.01006.x.
13. **McMichael AJ, Rowland-Jones SL.** 2001. Cellular immune responses to HIV. Nature **410:**980–987. http://dx.doi.org/10.1038/35073658.
14. **Doitsh G, Galloway NL, Geng X, Yang Z, Monroe KM, Zepeda O, Hunt PW, Hatano H, Sowinski S, Munoz-Arias I, Greene WC.** 2014. Cell death by pyroptosis drives CD4 T-cell depletion in HIV-1 infection. Nature **505:**509-514. http://dx.doi.org/10.1038/nature12940.
15. **Cookson BT, Brennan MA.** 2001. Pro-inflammatory programmed cell death. Trends Microbiol **9:**113–114. http://dx.doi.org/10.1016/S0966-842X(00)01936-3.
16. **Miao EA, Leaf IA, Treuting PM, Mao DP, Dors M, Sarkar A, Warren SE, Wewers MD, Aderem A.** 2010. Caspase-1-induced pyroptosis is an innate immune effector mechanism against intracellular bacteria. Nat Immunol **11:**1136–1142. http://dx.doi.org/10.1038/ni.1960.
17. **Brennan MA, Cookson BT.** 2000. Salmonella induces macrophage death by caspase-1-dependent necrosis. Mol Microbiol **38:**31–40. http://dx.doi.org/10.1046/j.1365-2958.2000.02103.x.
18. **Fink SL, Bergsbaken T, Cookson BT.** 2008. Anthrax lethal toxin and Salmonella elicit the common cell death pathway of caspase-1-dependent pyroptosis via distinct mechanisms. Proc Natl Acad Sci U S A **105:**4312–4317. http://dx.doi.org/10.1073/pnas.0707370105.
19. **Thirumalai K, Kim KS, Zychlinsky A.** 1997. IpaB, a Shigella flexneri invasin, colocalizes with interleukin-1 beta-converting enzyme in the cytoplasm of macrophages. Infect Immun **65:**787–793.
20. **McIlwain DR, Berger T, Mak TW.** 2013. Caspase functions in cell death and disease. Cold Spring Harb Perspect Biol **5:**a008656. http://dx.doi.org/10.1101/cshperspect.a008656.
21. **Xu H, Yang J, Gao W, Li L, Li P, Zhang L, Gong YN, Peng X, Xi JJ, Chen S, Wang F, Shao F.** 2014. Innate immune sensing of bacterial modifications of Rho GTPases by the Pyrin inflammasome. Nature **513:** 237–241. http://dx.doi.org/10.1038/nature13449.
22. **Ataide MA, Andrade WA, Zamboni DS, Wang D, do Carmo Souza M, Franklin BS, Elian S, Martins FS, Pereira D, Reed G, Fitzgerald KA, Golenbock DT, Gazzinelli RT.** 2014. Malaria-induced NLRP12/NLRP3-dependent caspase-1 activation mediates inflammation and hypersensitivity to bacterial superinfection. PLoS Pathog **10:**e1003885. http://dx.doi.org/10.1371/journal.ppat.1003885.
23. **Galloway NL, Doitsh G, Monroe KM, Yang Z, Munoz-Arias I, Levy DN, Greene WC.** 2015. Cell-to-cell transmission of HIV-1 is required to trigger pyroptotic death of lymphoid-tissue-derived CD4 T cells. Cell Rep **12:**1555-1563. http://dx.doi.org/10.1016/j.celrep.2015.08.011.
24. **Chen GY, Nunez G.** 2010. Sterile inflammation: sensing and reacting to damage. Nat Rev Immunol **10:**826–837. http://dx.doi.org/10.1038/nri2873.
25. **Lu W, Ma F, Churbanov A, Wan Y, Li Y, Kang G, Yuan Z, Wang D, Zhang C, Xu J, Lewis M, Li Q.** 2014. Virus-host mucosal interactions during early SIV rectal transmission. Virology **464-465:**406–414. http://dx.doi.org/10.1016/j.virol.2014.07.010.
26. **Li Q, Smith AJ, Schacker TW, Carlis JV, Duan L, Reilly CS, Haase AT.** 2009. Microarray analysis of lymphatic tissue reveals stage-specific, gene expression signatures in HIV-1 infection. J Immunol **183:**1975–1982. http://dx.doi.org/10.4049/jimmunol.0803222.
27. **Wu TD, Nacu S.** 2010. Fast and SNP-tolerant detection of complex variants and splicing in short reads. Bioinformatics **26:**873–881. http://dx.doi.org/10.1093/bioinformatics/btq057.
28. **Li H, Handsaker B, Wysoker A, Fennell T, Ruan J, Homer N, Marth G, Abecasis G, Durbin R.** 2009. The Sequence Alignment/Map format and SAMtools. Bioinformatics **25:**2078–2079. http://dx.doi.org/10.1093/bioinformatics/btp352.
29. **Thorvaldsdottir H, Robinson JT, Mesirov JP.** 2013. Integrative Genomics Viewer (IGV): high-performance genomics data visualization and exploration. Brief Bioinform **14:**178–192. http://dx.doi.org/10.1093/bib/bbs017.
30. **Anders S, Huber W.** 2010. Differential expression analysis for sequence count data. Genome Biol **11:**R106. http://dx.doi.org/10.1186/gb-2010-11-10-r106.
31. **Huang DW, Sherman BT, Lempicki RA.** 2009. Systematic and integrative analysis of large gene lists using DAVID bioinformatics resources. Nat Protoc **4:**44–57. http://dx.doi.org/10.1038/nprot.2008.211.
32. **Bedner E, Smolewski P, Amstad P, Darzynkiewicz Z.** 2000. Activation of caspases measured in situ by binding of fluorochrome-labeled inhibitors of caspases (FLICA): correlation with DNA fragmentation. Exp Cell Res **259:**308–313. http://dx.doi.org/10.1006/excr.2000.4955.
33. **Sloan RD, Kuhl BD, Mesplede T, Munch J, Donahue DA, Wainberg MA.** 2013. Productive entry of HIV-1 during cell-to-cell transmission via dynamin-dependent endocytosis. J Virol **87:**8110–8123. http://dx.doi.org/10.1128/JVI.00815-13.
34. **Barbalat R, Ewald SE, Mouchess ML, Barton GM.** 2011. Nucleic acid recognition by the innate immune system. Annu Rev Immunol **29:**185–214. http://dx.doi.org/10.1146/annurev-immunol-031210-101340.
35. **Gao D, Wu J, Wu YT, Du F, Aroh C, Yan N, Sun L, Chen ZJ.** 2013. Cyclic GMP-AMP synthase is an innate immune sensor of HIV and other retroviruses. Science **341:**903–906. http://dx.doi.org/10.1126/science.1240933.
36. **Jakobsen MR, Bak RO, Andersen A, Berg RK, Jensen SB, Tengchuan J, Laustsen A, Hansen K, Ostergaard L, Fitzgerald KA, Xiao TS, Mikkelsen JG, Mogensen TH, Paludan SR.** 2013. IFI16 senses DNA forms of the lentiviral replication cycle and controls HIV-1 replication. Proc Natl Acad Sci U S A **110:**E4571–E4580. http://dx.doi.org/10.1073/pnas.1311669110.
37. **Poltorak A, He X, Smirnova I, Liu MY, Van Huffel C, Du X, Birdwell D, Alejos E, Silva M, Galanos C, Freudenberg M, Ricciardi-Castagnoli P, Layton B, Beutler B.** 1998. Defective LPS signaling in C3H/HeJ and C57BL/10ScCr mice: mutations in Tlr4 gene. Science **282:**2085–2088. http://dx.doi.org/10.1126/science.282.5396.2085.
38. **Shi J, Zhao Y, Wang Y, Gao W, Ding J, Li P, Hu L, Shao F.** 2014. Inflammatory caspases are innate immune receptors for intracellular LPS. Nature **514:**187–192. http://dx.doi.org/10.1038/nature13683.
39. **Badley AD, Dockrell D, Simpson M, Schut R, Lynch DH, Leibson P, Paya CV.** 1997. Macrophage-dependent apoptosis of CD4+ T lymphocytes from HIV-infected individuals is mediated by FasL and tumor necrosis factor. J Exp Med **185:**55–64. http://dx.doi.org/10.1084/jem.185.1.55.
40. **Li Q, Duan L, Estes JD, Ma ZM, Rourke T, Wang Y, Reilly C, Carlis J, Miller CJ, Haase AT.** 2005. Peak SIV replication in resting memory CD4+ T cells depletes gut lamina propria CD4+ T cells. Nature **434:** 1148–1152.
41. **Mattapallil JJ, Douek DC, Hill B, Nishimura Y, Martin M, Roederer M.** 2005. Massive infection and loss of memory CD4+ T cells in multiple tissues during acute SIV infection. Nature **434:**1093–1097. http://dx.doi.org/10.1038/nature03501.
42. **Pantaleo G, Graziosi C, Demarest JF, Butini L, Montroni M, Fox CH, Orenstein JM, Kotler DP, Fauci AS.** 1993. HIV infection is active and

progressive in lymphoid tissue during the clinically latent stage of disease. Nature **362:**355–358. http://dx.doi.org/10.1038/362355a0.

43. **Whitney JB, Hill AL, Sanisetty S, Penaloza-MacMaster P, Liu J, Shetty M, Parenteau L, Cabral C, Shields J, Blackmore S, Smith JY, Brinkman AL, Peter LE, Mathew SI, Smith KM, Borducchi EN, Rosenbloom DI, Lewis MG, Hattersley J, Li B, Hesselgesser J, Geleziunas R, Robb ML, Kim JH, Michael NL, Barouch DH.** 2014. Rapid seeding of the viral reservoir prior to SIV viraemia in rhesus monkeys. Nature **512:**74–77. http://dx.doi.org/10.1038/nature13594.
44. **Satoh T, Kato H, Kumagai Y, Yoneyama M, Sato S, Matsushita K, Tsujimura T, Fujita T, Akira S, Takeuchi O.** 2010. LGP2 is a positive regulator of RIG-I- and MDA5-mediated antiviral responses. Proc Natl Acad Sci U S A **107:**1512–1517. http://dx.doi.org/10.1073/pnas.0912986107.
45. **Brenchley JM, Price DA, Schacker TW, Asher TE, Silvestri G, Rao S, Kazzaz Z, Bornstein E, Lambotte O, Altmann D, Blazar BR, Rodriguez B, Teixeira-Johnson L, Landay A, Martin JN, Hecht FM, Picker LJ, Lederman MM, Deeks SG, Douek DC.** 2006. Microbial translocation is a cause of systemic immune activation in chronic HIV infection. Nat Med **12:**1365–1371.
46. **Dyavar Shetty R, Velu V, Titanji K, Bosinger SE, Freeman GJ, Silvestri G, Amara RR.** 2012. PD-1 blockade during chronic SIV infection reduces hyperimmune activation and microbial translocation in rhesus macaques. J Clin Invest **122:**1712–1716. http://dx.doi.org/10.1172/JCI60612.
47. **Li Q, Estes JD, Duan L, Jessurun J, Pambuccian S, Forster C, Wietgrefe S, Zupancic M, Schacker T, Reilly C, Carlis JV, Haase AT.** 2008. Simian immunodeficiency virus-induced intestinal cell apoptosis is the underlying mechanism of the regenerative enteropathy of early infection. J Infect Dis **197:**420–429. http://dx.doi.org/10.1086/525046.
48. **Estes JD, Harris LD, Klatt NR, Tabb B, Pittaluga S, Paiardini M, Barclay GR, Smedley J, Pung R, Oliveira KM, Hirsch VM, Silvestri G, Douek DC, Miller CJ, Haase AT, Lifson J, Brenchley JM.** 2010. Damaged intestinal epithelial integrity linked to microbial translocation in pathogenic simian immunodeficiency virus infections. PLoS Pathog **6:**e1001052. http://dx.doi.org/10.1371/journal.ppat.1001052.